

## Geology and Geothermal Systems in the Bajawa Volcanic Rift Zone, Flores, Eastern Indonesia

Hiroyuki Muraoka\*, Asnawir Nasution, Janes Simanjuntak, Sjafra Dwipa, Masaaki Takahashi, Hiroshi Takahashi, Koji Matsuda and Yoshikazu Sueyoshi

\*Institute for Geo-Resources and Environment, AIST, Central 7, Higashi 1-1-1, Tsukuba, Ibaraki 305-8567, Japan

\*hiro-muraoka@aist.go.jp

**Keywords:** Indonesia, Flores, Bajawa, Mataloko, geothermal heat source, volcanic rift zone, monogenetic volcano, geothermal system, vapor-dominated geothermal system.

### ABSTRACT

An Indonesia-Japan bilateral research cooperation project has been carried out in Bajawa City and its surrounding areas, Flores Island, Indonesia, from 1997 to 2002. Regional tectonic setting of the Bajawa geothermal field is characterized by the NNW-SSE left-lateral shear stress accommodated between the north-moving Australia continent in the east and relatively stable "Sundaland" continent in the west. In accordance with this stress regime, an inner volcanic arc of Lesser Sunda Islands forms en echelon volcanic islands. Each echelon element shows a combination of a large-scale anticline of volcanic basement units and overlying a cluster of young volcanoes. If a concept of mantle diapir is assumed, geneses of a large-scale anticline and a cluster of volcanoes can be explained at the same time. The Bajawa volcanic rift zone consists of 60 monogenetic breccia cone volcanoes along the NNW-SSE trending zone, each of which was derived from the phreato-magmatic eruption. Genesis of each cone probably corresponds to each dike-filling event at a depth. A small phreato-magmatic eruption occurred at one of the summits, January 2001, having formed a fissure at the surface. This suggests that an upper tip of the dike reached very shallow-depth near the surface, characterizing that the geothermal heat sources are small, but numerous, shallow and very active in the Bajawa rift zone. These cones are composed of homogeneous calc-alkaline andesite and their phase relation indicates that the magma were derived from a depth of ca. 10 km near the bottom of the immature crust in this region. Three steaming grounds, Mataloko, Nage and Bobo, are known along the Bajawa rift zone with many hot springs. The well MT-2 was drilled to a depth of 162.35 m in the Mataloko steaming ground and constantly produced 15 tons per hour of dry steam. A temperature profile estimated from phase analyses of cutting samples shows that the field is characterized by a vapor-dominated geothermal system. Most areas of the Bajawa rift zone seem quite prospective on the geothermal potential, because of the ubiquitous heat sources and uniform hydrological settings.

### 1. INTRODUCTION

For the purpose of contribution to the Rural Electrification Program in Indonesia, a five-year Indonesia-Japan bilateral international research cooperation project named "Research Cooperation Project on the Exploration of Small-scale Geothermal Resources in the Eastern Part of Indonesia" has been carried out from 1997 to 2002. Bajawa City and its surrounding areas, central Flores Island, were selected for the study area. The study area is defined as the onshore zone transecting central Flores Island from north to south

that are bounded by 120° 52' 30" E-121° 07' 30" E and 8° 22' 30" S-8° 58' 00" S (Fig. 1).

From the volcanological point of view, it is of great interest that Quaternary volcanoes are distributed along the volcanic front with 60 or 70 km spacing in western Indonesia from Sumatra to Lombok or Sumbawa Islands, whereas the spacing abruptly reduces to the half in eastern Indonesia from Flores to Pantar Islands. This contrast may be related to the fact that the Flores-Pantar segment is specified by the en echelon volcanic islands (Muraoka et al. 2002a). The tight spacing of volcanoes brings us an advantage for the rural geothermal electrification, providing ubiquitous geothermal resources over this segment.

The southern half of the study area has been noticed for a long time from the viewpoint of geologic remote sensing because the remote sensor imagery presents numerous spectacular volcanic craters resembling the surface of the Moon (e.g., Muraoka, 1989). Through the project, we have recognized that they are composed of about 60 monogenetic volcanoes, bringing major geothermal activities in the study area such as the steaming grounds in Bobo, Nage and Mataloko, and the voluminous hot spring discharge in Mengeruda.

A phreato-magmatic eruption occurred at the Inie Lika volcano during the project, January 11-16, 2001 after 95 years of quiescence (Muraoka et al., 2002b). It reminds us that the major geothermal resources in the study area are associated with an active volcanic system.

Shallow exploratory wells have been drilled in the Mataloko field during this project. One of the wells drilled to a depth of 162.35 m produced 15 tons per hour of dry steam (Sueyoshi et al., 2002). Mineralogical analyses on the cutting samples have been made.

This paper describes outline geology and geothermal systems in the Bajawa geothermal field, integrating various data obtained through this project, particularly focusing to its specific geothermal heat source named Bajawa rift zone.

### 2. TECTONICS

The Sunda-Banda arc spans 4,300 km from Sumatra Island in the west through Kai Islands in the east to Buru Island in the north (Fig. 2). This arc is broadly divided into two contrasting sectors: the Greater Sunda sector in the west and Lesser Sunda-Banda sector in the east (Fig. 2). The Greater Sunda sector is said to be an active continental margin because the arc is situated at the southern front of a broad continent called "Sundaland" mainly concealed under shallow seawater (Fig. 2). The subducting Indian Plate basically consists of the oceanic crust in the Greater Sunda sector.

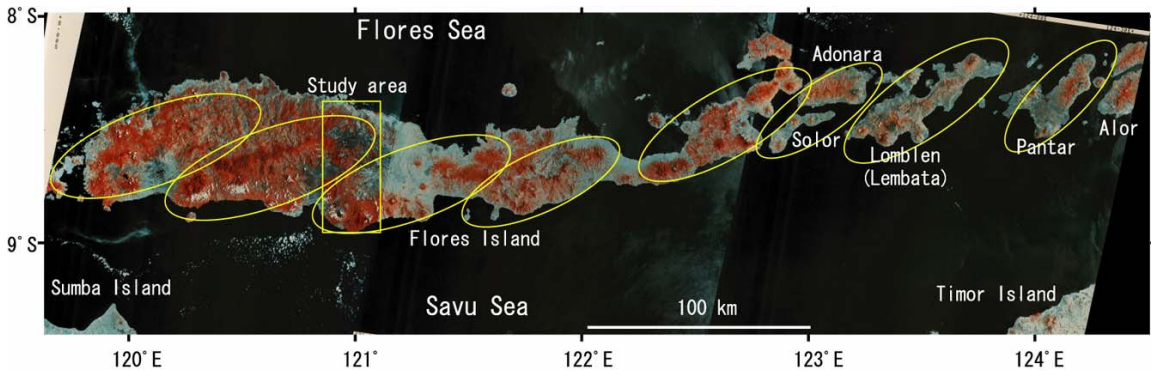


**Figure 1:** Landsat MSS imagery on the inner Lesser Sunda arc. Note the en echelon shaped topographic structure in this sector of the Lesser Sunda arc. Each element of en echelon structure consists of a culmination of the anticline and clustered young volcanoes.

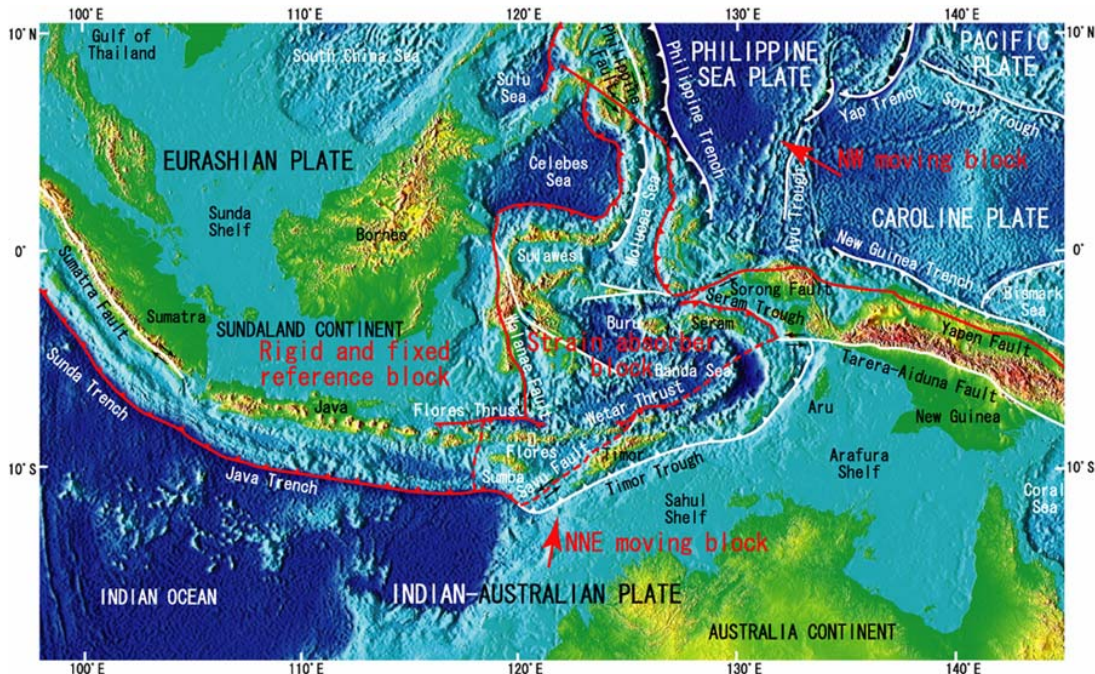


**Figure 2:** Tectonic map of Indonesia and its surrounding areas. An on-line global relief image ETOPO2 (Global 2-min gridded data) was used as a base map from the National Geophysical Data Center (NGDC), NOAA. White lines show the ordinary plate boundaries and major faults, whereas red lines show the estimated boundaries of four tectonic blocks with different motions based on the current GPS data. GPS measurements show that Indian-Australian Plate is moving NNE and Pacific Plate is moving NW with respect to Eurasian Plate, so that the internal block plays a role of a strain absorber to the surrounding three major plates. As a result, the Banda arc is still bending and Flores Island is subject to the NNW-SSE trending left-lateral shear stress.

This combination allows a stable subduction regime in the sector. The Lesser Sunda-Banda sector is an immature island arc with marginal seas of oceanic crust behind it such as the Flores Sea and Banda Sea. A subducting plate consists of the Australia continent in the Lesser Sunda-Banda arc so that the buoyant lithosphere is underplating less buoyant lithosphere resulting in unstable subduction or collision tectonics.

## 2.1 Regional Tectonic Settings

Based on a map of the GPS relative motions by Kreemer et al. (2000), a region of Fig. 2 can be subdivided into four tectonic blocks, which are bounded by red color lines, in terms of motions: (1) A block of Sundaland and its eastern margins are apparently coherent in motions so that the motions are here assumed to be fixed to other blocks as a reference, (2) A block of Indian-Australian Plate and its northern accretions are moving north or NNE, (3) A block of Pacific-Caroline-Philippine Sea Plate and its western accretions are moving WNW or northwest and (4) An

internal block including Flores, Banda Sea and Sulawesi plays a role of a strain absorber where the strains given from the surrounding blocks are almost absorbed within this block as its internal deformations. In other words, most deformations are concentrated in the Flores-Banda-Sulawesi block. In the Flores-Banda-Sulawesi block, the northern part is subject to the motion of the Pacific block and the southern part is subject to the motion of the Indian-Australian block. As a result, the block is rotating counter-clockwise even now. This suggests that the counter-clockwise bending of the Banda arc is still ongoing.

## 2.2 En Echelon Array in the Lesser Sunda Islands

Fig. 1 shows three scenes of Landsat MSS imagery in a part of the inner Lesser Sunda Islands from Flores to Pantar Islands. This part of the arc distinctively forms en echelon volcanic islands and becomes obscured to the east and west.

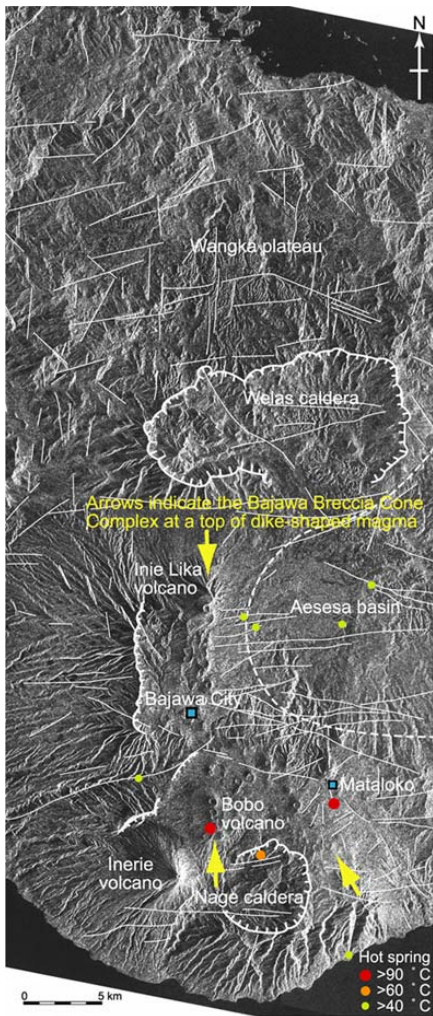


**Figure 3: JERS-1 SAR Imagery of the study area acquired on February 3, 1996 (Copyright METI/NASDA). Extracted lineaments, calderas, walls of the rift zone and other features are shown.**

Each element of en echelon forms topographically an elongated dome with an ENE-WSW trending axis and about 90 km by 30 km area that is composed both of a culmination of an anticline and cluster of young volcanoes as described below. Island itself sometimes coincides with an element of the en echelon structure such as Lomblen and Pantar Islands.

Generally, en echelon volcanic islands are common in the oblique subduction zone like the Kuril and Aleutian arcs, where the direction of the subduction tends to be perpendicular to the anticline axes of each echelon element. However, the direction of the subduction is NNE for the inner Lesser Sunda Islands and an array of en echelon elements is opposite to this direction. This requires another explanation for the formation process other than the oblique subduction.

Again, GPS measurements provide a clue to this problem. As shown in Fig. 2, the outer Lesser Sunda Islands including Timor Island seem almost accreted to the Indian-Australian Plate in terms of motions, where the estimated Savu Fault (Rutherford et al., 2001) is a possible block boundary rather than the Timor Trough. As a result, the en echelon sector from Flores to Pantar Islands is a place for the shear strain absorber between the Sundaland block and Indian-Australian block, where the western tip is rather

fixed relative to the Sundaland block but the eastern tip is subject to the north-moving Indian-Australian block. A force of this left lateral shear stress in the NNW-SSE direction or anticlockwise moment might have caused the array of en echelon islands in a limited part of the inner Lesser Sunda sector.

### 3 GEOLOGY OF EN ECHELON STRUCTURE

Numerous volcanic craters are known in the Bajawa area as shown in Fig. 3. This area was selected as a model field in the Indonesia-Japan geothermal project because of the presence of many steaming grounds in their vicinity, and geological survey was carried out in this project. Figure 4 shows the result of geological mapping. This area includes eastern and western edges of two echelon elements as a part of the echelon islands as seen in Fig. 1. General geology was described in detail in Muraoka et al. (2002a), and will be given here on the two topics, two large anticlines corresponding to two elements of en echelon volcanic islands and young volcanoes in this field.

#### 3.1 Anticlines of the Volcanic Basement Units

Two anticlines are shown in the map and the A (north)-B (south) cross-section of Fig. 4. Northern one is situated in northern rim of Welas caldera that is named here Welas anticline. Southern one is situated in Mataloko area that is named here Mataloko anticline. Both of them are gentle and broad anticlines covering 20 km from the north wing to south one. Therefore, hinge lines are difficult to determine. Volcanoes are concentrated on these anticlines. Both of terrains show parts of two elements of the en echelon island structure characteristic from Flores to Pantar Islands (Fig. 1). These anticlines well reflect the present topography. The reason is ascribed to their younger origins as mentioned below.

The oldest exposed unit is the Middle Miocene (ca.16.2-10.2 Ma) Nangapanda Formation that is exposed in the northern area. The Nangapanda Formation is submarine sediments composed of shale, sandstone, chert, limestone and pumice tuff. After relatively a long time hiatus, lava flow volcanism of the Wangka Andesite and Maumbawa Basalt widely occurred in a subaerial environment during 4-3 Ma. Probably, Lesser Sunda Islands might have first appeared above sea level at this stage because subaerial Miocene strata have seldom been reported from this region. Afterward, a marine transgression occurred. This marine transgression was smaller than that of the Miocene but was the largest since the Pliocene. Low altitude areas were invaded by seawater. At 2.5 Ma in the peak stage of the marine transgression, the Welas caldera collapsed and produced the voluminous Welas Tuff that was dated to be 2.5 Ma by K-Ar age measurements (Muraoka et al., 2002a).

The Welas Tuff was deposited in a marine environment south of the present Mataloko anticline and north of the present Welas anticline. The tuff was also deposited in a lacustrine environment called the Aesesa basin between the two anticlines (Fig. 4). Successively after the Welas Tuff, three units, the Waebela Basalt, Aesesa Formation and Matale Limestone, were deposited in a marine environment south of the Mataloko anticline, lacustrine environment at the Aesesa basin and marine environment north of the Welas anticline, respectively. These three units are the contemporaneous heterotopic facies in a broad sense.

Presently the highest distribution of the Matale Limestone is 900 m and hyaloclastite of the Waebela Basalt is 900 m above sea level.

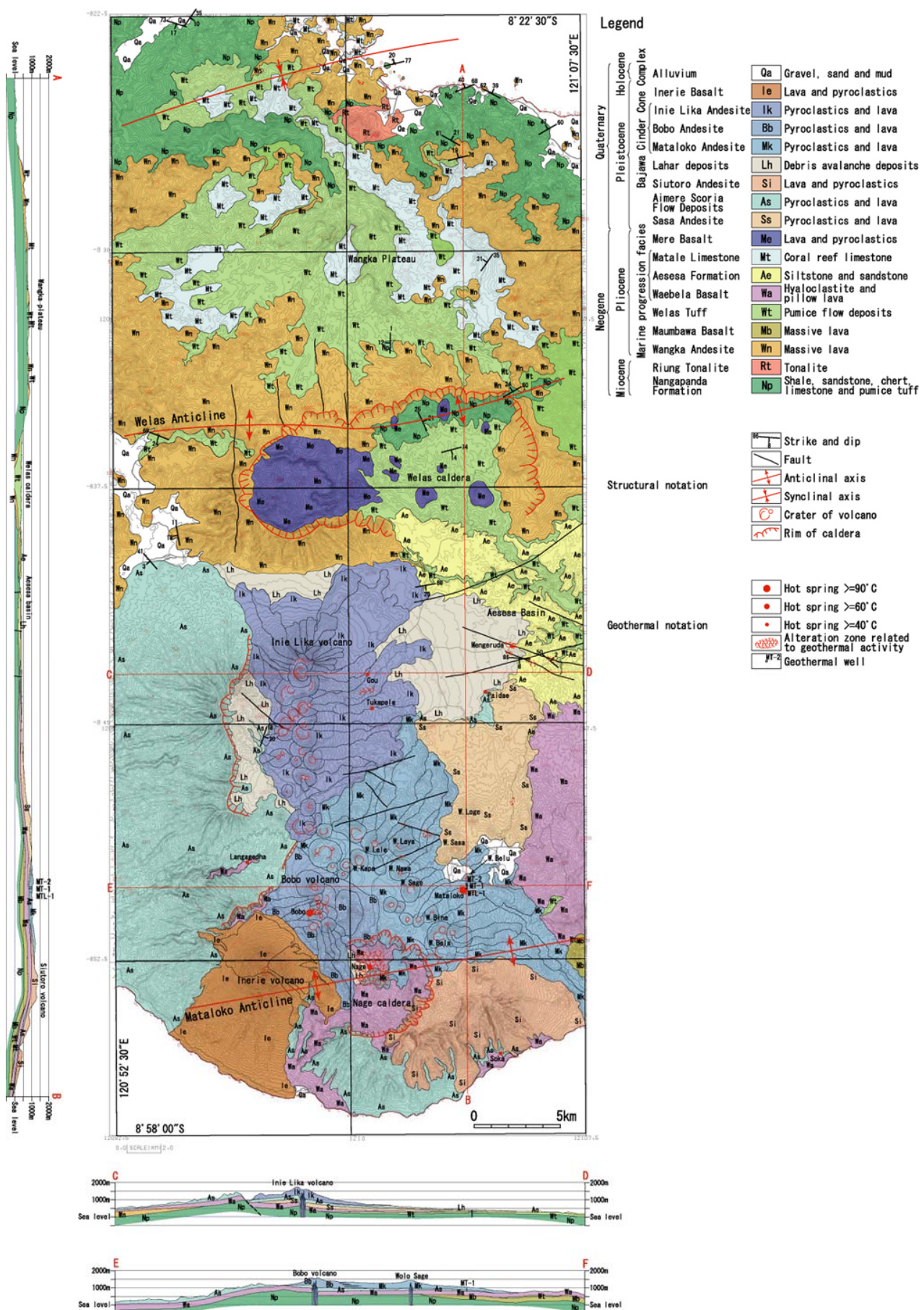


Figure 4: Geological map and geological cross sections of the study area, central Flores, Indonesia.

Some part of this marine transgression at around 2.5 Ma could be ascribed to the global eustatic changes of sea level. Marine tuff with about 2.5 Ma age was actually reported from high altitude area of Lomblen Island (Muraoka, 1989) and the marine transgression at 2.5 Ma has been reported from Northeast Japan (Muraoka and Takakura, 1988). Eustatic change of sea level can, however, explain only a hundred meters of sea level rise at the maximum since the Miocene (Vail and Hardenbol, 1979). In other words, the Matale Limestone and the Waebela Basalt at 900 m above sea level suggest that, if 100 m of sea level rise is assumed, the rest 800 m uplift was derived from the anticline-forming tectonics near the anticline axes. High altitude distribution of the Matale Limestone and hyaloclastite of the Waebela Basalt are, in fact, found near the Welas anticline and the Mataloko anticline, respectively. This means that the average uplifting rate of two anticlines is 0.32 mm/year during the past 2.5 million years.

### 3.2 Clustered Volcanoes on the Anticlines

Volcanoes on the two anticlines will be here described. On the Welas anticline, the Welas caldera formed at about 2.5 Ma. The Mere Basalt, forming post-caldera volcanoes, was not dated but may be the latest Pliocene or early Quaternary in age judging from stratigraphy to other dated units. After the post-caldera volcanism, the volcanic activity has been almost extinct. Therefore, after these events, volcanism is not found on the Welas anticline in the area of Fig. 4. However, a major part of this en echelon element is extending to the western outside of Fig. 4 and several Quaternary volcanoes are known (Nasution et al., 2002). Particularly, they includes Ranakah volcanoes south of Ruten City where the Directorate of Volcanology and Geological Hazard Mitigation defined as an active volcano and placed an observatory (Nasution et al., 2002). Anak Ranakah volcano (anak means children in Indonesian), one of them, has abruptly appeared in 1987 as a new lava dome.

On the Mataloko anticline, volcanic activity has continued from 4 Ma to the present, and this terrain is almost entirely covered by the Pliocene and Quaternary volcanic rocks. Several late Quaternary volcanoes are recognized on the Mataloko anticline. Inerie volcano lies near the southwestern coast and forms a typical stratovolcano (Figs. 3 and 4). Fumarolic activity is sometimes observed at the summit crater. Ebulo volcano lies at the eastern outside of Fig. 4 and forms a typical stratovolcano. Strong fumarolic activity at the summit crater is always seen from far a way. The Inie Lika volcano is situated immediately north of Bajawa, a capital city of Ngada District, and composed of about 25 breccia cones over 10 km in the NNW-SSE direction (Fig. 4). To the south, there is Bobo volcano that is also composed of about 10 breccia cones. Both Inie Lika and Bobo volcanoes are traditionally distinguished because of the isolation of the major volcanic edifices. However, Fig. 3 shows that small breccia cones are also aligned between them and all the elements form an almost continuous alignment over 20 km. To the southeast, two rows of NW-SE trending breccia cone alignments are also found as other branches that contain about 25 breccia cones (Fig. 4). All the breccia cone alignments seem to reflect a connective dike complex at a depth. Their lithology and eruption mode of breccia cones are similar to each other. Although the precise age seems slightly younger toward the north as shown by the historic eruption records in the northern Inie Lika volcano in 1905 and 2001 (Muraoka et al., 2002b), these cones occupy almost the same stratigraphic horizon (Fig. 4). Therefore, regardless of the isolation of volcanic edifices, they seem cognate in their origin and are called the Bajawa Cinder Cone Complex

(Muraoka et al., 2002a). However, fragments consisting these cones are unusually non-porous compared to other monogenetic volcanoes and the term "Cinder Cone" or "Scoria Cone" is not adequate. Then, the name is revised to be Bajawa Breccia Cone Complex in this paper. The age of the Bajawa Breccia Cone Complex is estimated to be younger than 160 Ka by Takashima et al. (2002) by the thermoluminescence dating method. The latest eruptions occurred in the complex at 1905 and 2002.

### 3.3 Origin of the En Echelon Volcanic Arc and Mantle Diaps

The Flores to Pantar segment of the Lesser Sunda arc is characterized by the en echelon volcanic islands. Each element of en echelon volcanic islands shows a topographically elongated dome with an ENE-WSW trending axis and about 90 km by 30 km area that consists of two structures: culmination of the WSW-ENE anticline of volcanic basement units and overlying clustered young volcanoes. These anticline axes are not perpendicular to the NNE-SSW plate motion of the subducting Australian Plate, but perpendicular to the NNW-SSE left-lateral shear stress accommodated between north-moving Australian continental accretions in the east and relatively fixed Sundaland in the west. Geological mapping was carried out in part of the echelon segment, and shows that two anticline axes corresponding to two echelon elements reveal 800 m uplift during the last 2.5 million years. This large uplifting could explain the fact that the elongated dome of en echelon volcanic islands sometimes coincides with each island itself. First, genesis of these anticline axes should be explained. Another feature of en echelon volcanic islands is that young volcanoes are clustered on the culmination of these anticline axes. Second, genesis of these clustered young volcanoes should be explained. Geneses of anticline axes and clustered young volcanoes are tectonic and magmatic processes, respectively. Third, these different processes that were localized in the same areas should be explained.

The tectonic and magmatic processes are different categories and their co-existence in the same area is generally difficult to be explained. However, if we introduce a concept of mantle diaps, these phenomena could be systematically explained. Figure 5 shows a model of mantle diaps explaining these questions. As known in the original concept of mantle diaps, mantle diaps would release ascending magma bodies toward shallower crust resulting in clustered volcanoes at the surface. At the same time, the top of mantle diaps forms high-temperature (1000~1300 °C) thermal fields near the depth of Moho discontinuity (Tatsumi, 1989), shifting a brittle-plastic transition (350~400 °C) toward a shallow depth. In addition, high-level magma chambers generated from mantle diaps would also make the brittle-plastic transition shift toward a very shallow depth. This was demonstrated by a borehole in the Kakkonda geothermal field, Japan, where the brittle-plastic transition is observed only at a depth of 3.1 km (Muraoka et al., 1998), although the precise discussion needs a precise definition for the brittle-plastic transition. Therefore, the brittle layer above mantle diaps could be very thin and they are easily deformed. If the thin part of the brittle layer suffered with a simple lateral shear, they could be not only deformed laterally but also uplifted by the buoyancy of plastic layers toward the free surface, forming elongated domes. It is also noted that, when plastic-brittle layers are deformed, the brittle layer is subjective and the plastic layer is passive as seen in folding processes of the multi-layer system. The shape of mantle diaps is subjected to the deformation of the overlying

brittle layer. For this requirement, the bottom of the brittle layer is drawn at a relatively shallow level in Fig. 5 for visual convenience, but it must reach the deeper level to the surroundings of the mantle diapirs. Thus, an assumption of mantle diapirs simultaneously explains all the questions concerned.

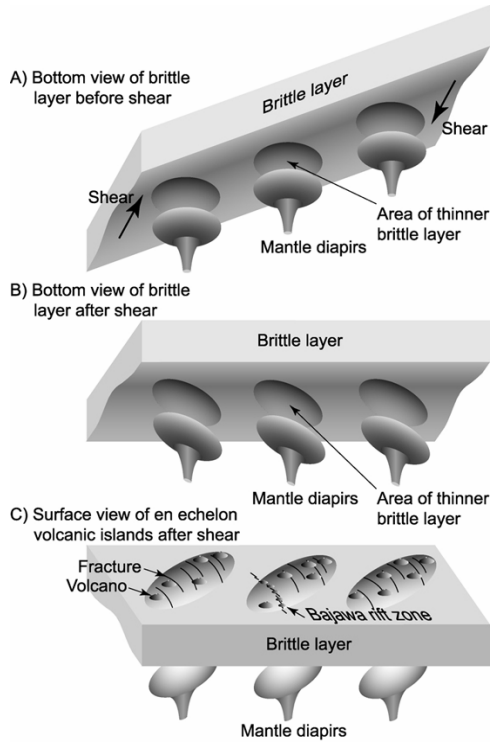


**Figure 5: Schematic diagrams for the formation of en echelon volcanic islands by a chain of mantle diapirs. A) Bottom view of brittle layer before shear. B) Bottom view of brittle layer after shear. C) Surface view of en echelon volcanic islands after shear.**

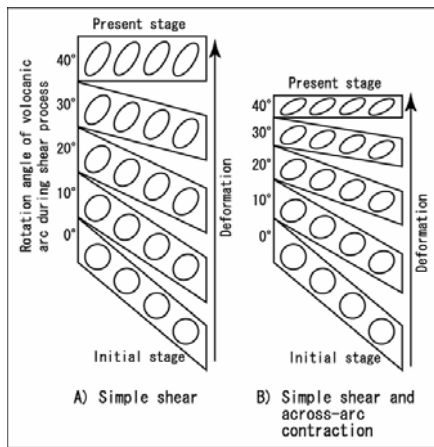


**Figure 6: Geometrical control of deformation of the volcanic arc and the area of thinner brittle layer in plan view. Initial shape of the area of thinner brittle layer assumed to be circular in plan. A) Case of simple shear. B) Case of simple shear and across-arc contraction where the final contraction is 50 % across arc.**

Figure 6 shows a simple geometrical consideration on the lateral deformation on the thinner parts of brittle layers above mantle diapirs. We shall assume that the thinner parts of brittle layers above mantle diapirs are originally circular in plan. In this case, even if we deform them by the simple

shear, we cannot get the required geometry as seen in Fig. 1 where the axis of elongated dome has low angle to the axis of the island arc. To get the required geometry as seen in Fig. 1, we must add across-arc contraction deformation up to 50 % in addition to the simple shear. Folding structures themselves observed in Bajawa show the presence of the across-arc contraction but other contributions by such as reverse faults and strike-slip faults could be required.

Muraoka et al. (2002a) called the zone of the Bajawa Breccia Cone Complex the Bajawa rift zone. They thought that it was some sort of “volcanic rift zone” defined by Walker (1999) where the left-lateral shear stress was liberating. The source magma of the rift zone was derived from about 10 km depth near the bottom of the crust in this region as described below. When we re-interpret these ideas from the present standpoint on the mantle diapir, it can be said as follows. The Bajawa rift zone is ascribed to a fracture appeared in the thinner part of the brittle layer of crust above a mantle diapir by the left-lateral shear. The pressure drop along the fracture and the high-temperature thermal field above the subsurface mantle diapir made the lower oceanic crust partially fused and generated the dike swarm (Muraoka et al., 2002c). The reason why the Bajawa rift zone is not continued to the north and south like the mid-ocean ridge is explained by the limited extent of the subsurface mantle diapir (Fig. 5C).

The Bajawa Breccia Cone Complex is not only clustered volcanoes, but also typical monogenetic volcanoes, each of which occurs at an arbitrary place in the Bajawa rift zone. Localization of the monogenetic volcanoes is one of enigma until now, but the recognition of mantle diapir in the Bajawa Breccia Cone Complex would provide us a clue to the genesis of the monogenetic volcanoes.

Tomiya (1991) thought that a mantle diapir corresponds to a single composite volcano at the surface and its span of life is a several hundreds thousand years. However, from the viewpoint of the present paper, a mantle diapir could correspond to clustered volcanoes in the area of 90 km by 30 km and its span of life could at least reach 2.5 million years. For example, closely packed five calderas occurred in the limited area of 40 km by 40 km in the Hakkoda volcanic field, Japan, and their span of life reaches 3.5 million years (Muraoka and Takakura, 1988). This may also represent an example of a manifestation of a single mantle diapir.

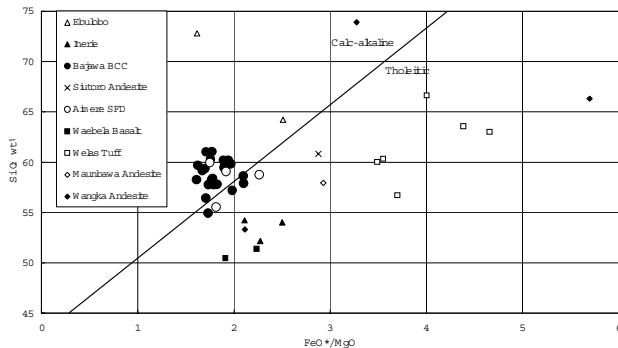
#### 4. MAGMA GENESIS

##### 4.1 Homogeneity of the Bajawa Rift Zone Magmatism

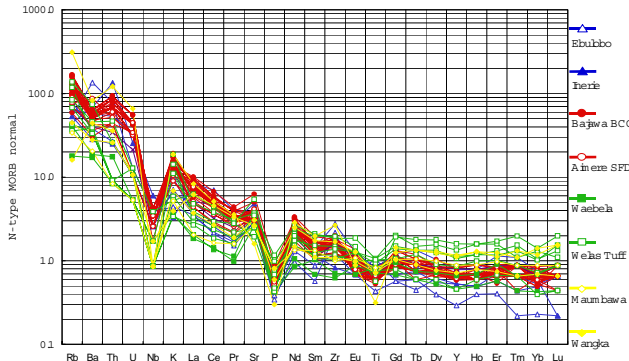
Forty-four volcanic rock samples were analyzed (Muraoka et al., 2002c). Four samples were taken from the Aimere Scoria Flow Deposits and 22 samples were taken from the Bajawa Breccia Cone Complex (the Mataloko Andesite, Bobo Andesite and Inie Lika Andesite) so that 26 samples represent the Bajawa rift zone volcanism. Porous samples are not rare and more or less hydrated. For this reason, anhydrous basis recalculation was made including minor elements before the plot on the following diagrams.

Figure 7 shows the  $\text{SiO}_2\text{-FeO}^*/\text{MgO}$  diagram. It is noteworthy that the chemical features of the Aimere Scoria Flow Deposits (0.8-0.2 Ma) are almost the same as the Bajawa Breccia Cone Complex in spite of the difference of their ages. This proposes a concept that the Bajawa rift zone volcanism was composed not only of the activity of the Bajawa Breccia Cone Complex but also the pre-existing elongated volcano. Therefore, the Aimere Scoria Flow

Deposits and the Bajawa Breccia Cone Complex are called the Bajawa rift zone volcanic rocks hereinafter. The Bajawa rift zone volcanic rocks are quite homogeneous compared to their spatial extent, while other units are heterogeneous on the diagram. Most units are scattered and rather dominant in the tholeiitic field. However, the Bajawa rift zone volcanic rocks form a confined cluster in the calc-alkaline field. Empirically and theoretically, calc-alkaline magma tends to rise to a shallower depth due to its buoyancy and play a major role for the geothermal heat sources in continental crust regions (Muraoka, 1997). Actually, most geothermal manifestations in the study area are closely associated with the Bajawa rift zone (Fig. 4) and indicate that the Bajawa rift zone is the major geothermal heat sources in the study area.



**Figure 7: The  $\text{SiO}_2$ - $\text{FeO}^*/\text{MgO}$  diagram of 44 volcanic rock samples in the Bajawa geothermal field. The thick line shows the boundary of the tholeiitic and calc-alkaline series by Miyashiro (1974).**



**Figure 8: The N-type MORB normalized diagram of 44 volcanic rock samples in the Bajawa geothermal field.**

Figure 8 shows the N-type MORB-normalized diagram. All the rocks show a typical island-arc pattern with a strong enrichment of incompatible elements (left side of the diagram) and dips of high field strength elements (e.g., Nb and Ti). The homogeneity of the Bajawa rift zone volcanic rocks (red) is again prominent. They occupy 60 % of analyzed samples, nevertheless, their extent is confined to a narrower zone compared to other units. When we subdivide all the volcanic rocks into the Bajawa rift zone volcanic rocks (red), the units older (yellow and green) and units younger (blue) than these rocks, the MORB-normalized patterns show that the incompatible elements become enriched and compatible elements become depleted with age. This may be explained by the decreasing degree of partial fusion with the change from an enriched mantle to a

depleted mantle since the collision of the Australia continent. It is at least clear that the Bajawa rift zone volcanic rocks are quite homogeneous not only in major elements but also minor elements, suggesting their cognate origin. One of the most probable models is a connected dike complex that is derived from the Bajawa rift zone (Fig. 9). The magma has likely been produced by the partial fusion under a constant physical condition during the past 0.8 million years.

#### 4.2 A possible shallow source of the Bajawa rift zone magmatism

In the last two decades, pseudoternary phase diagrams have been often used on the mid-ocean ridge basalt and some researchers have expanded the diagrams to the silicic region (Baker and Eggler, 1983, 1987) where Pl is plagioclase, Ol is olivine, and SiOr is quartz + orthoclase components. We try to apply these methods to the Bajawa rift zone volcanic rocks. Only 26 samples of the Bajawa rift zone volcanic rocks are treated because volcanic rocks of other units have a wide variety in composition.

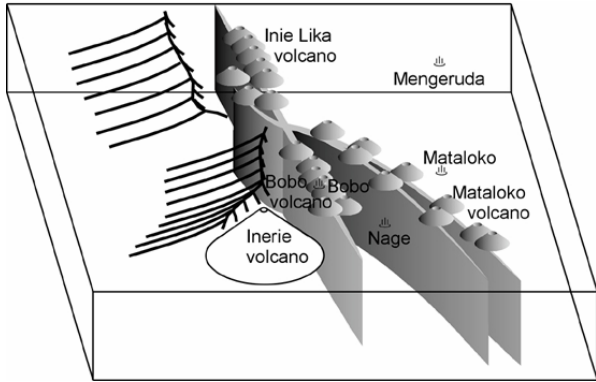
Fig. 10 shows the Di-Ol-SiOr pseudoternary diagram of 26 Bajawa rift zone volcanic rock samples where Di is a diopside component. On this diagram, the cluster seems to be situated between 5 kbar and 2 kbar, particularly two samples at the dioxide poor end seem to trace a phase boundary between the olivine and orthopyroxene fields. Another information on this diagram is that if the magma represented by the cluster is driven from a higher-pressure condition at 4 or 3 kbar to 2 kbar, the magma settles in the olivine-initial field even in silicic compositions. This may explain the reason why olivine phenocrysts are common in the Bajawa rift zone volcanic rocks even in andesite compositions.

Fig. 11 shows the Pl-Di-SiOr pseudo-ternary diagram of 26 Bajawa rift zone volcanic rock samples. This diagram seems to identify the pressure condition, that is, the equilibrium pressure is confined between 5 and 2 kbar. The extent of silica poor side is rather close to 2 kbar. However, we realize that the pressure may not be exactly 2 kbar from Fig. 10. Therefore, 3 kbar may be adopted as the equilibrium pressure on the Bajawa rift zone magma.

The estimated pressure of 3 kbar is only about 10 km in depth. The depth may normally be ascribed to the depth of a magma chamber. However, if there exists a magma chamber at a 10 km depth, fractional crystallization inevitably occurs resulting in the heterogeneity of the magma. The homogeneity should be maintained only when the dike swarm rapidly rises from the magma source region. A subsurface dike swarm estimated from linear alignments of the Bajawa Breccia Cone Complex also suggests rift-type magmatism along a tectonic line that is incompatible with the magma chamber (Fig. 9). The homogeneity of magma, a possible dike swarm and the presence of the rift zone are all features indicating that a depth of 10 km is rather ascribed to the magma source region. One may doubt the depth for a magma source region of the Bajawa rift zone volcanic rocks. If we consider common-type subduction magmatism, a greater depth will be required as a magma source region even at a volcanic front. However, although the Bajawa rift zone is a small-scale rift in the contraction tectonic field, this zone is situated in the NNW- SSSE trending left-lateral shear stress region constrained by the plate interactions (Muraoka et al., 2002a). In the mid-ocean ridges, recent topics are the shallow-depth magmatism. If rift type magmatism is adopted, the 10 km depth is not surprisingly shallow as a magma source region. Another

constraint is that the thickness of continental crust is estimated to be only 5 km in the Flores Island area (Curray et al., 1977). When we assume the thickness of the underlying oceanic crust is 7 km from the earth's average, a total crust thickness for Flores Island is only 12 km. Therefore, the Bajawa rift zone magma may be derived from the partial fusion of the bottom of the oceanic crust.

We consider that the shear stress concentration has generated the left-lateral en echelon fractures and formed a rift zone. The rifting activity might have produced abundant tholeiitic basalt magma from the upper mantle such as the Waebela Basalt, a considerable part of which might have been accommodated at the Moho discontinuity. Their heat might have caused partial fusion of the oceanic crust bottom that could be the source of the calc-alkaline magma in the Bajawa rift zone. The homogeneity of the Bajawa rift zone volcanic rocks is thus ascribed to its short pass from the magma source region at a 10 km depth to the surface and its non-stop rising as a dike swarm.



**Figure 9: Schematic model of connected dikes beneath the Bajawa Breccia Cone Complex (Muraoka et al., 2002a).**

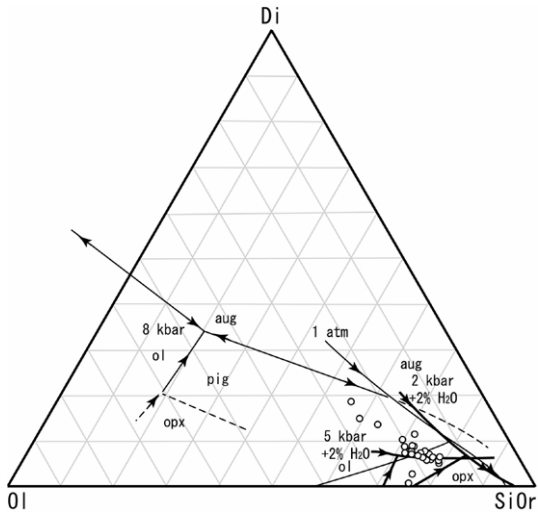


**Figure 10: The Di-Ol-SiOr pseudo-ternary diagram of 26 Bajawa rift zone volcanic rock samples. Phase relations were determined by Baker and Eggler (1987).**

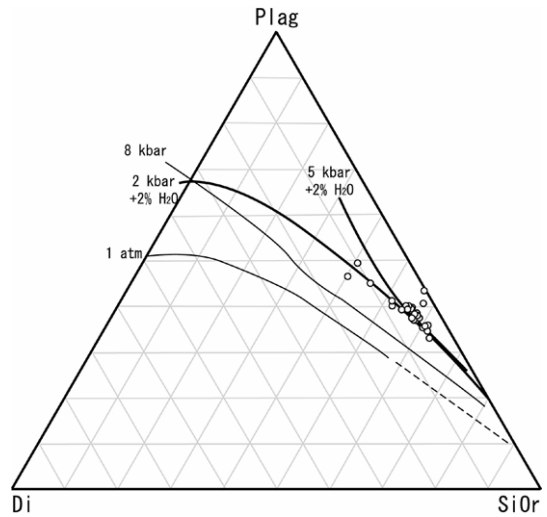


**Figure 11: The Plag-Di-SiOr pseudo-ternary diagram of 26 Bajawa rift zone volcanic rock samples. Phase relations were determined by Baker and Eggler (1983).**

## 5. FLUID GEOCHEMISTRY

Fluid geochemistry in the study area has been described in detail by Takahashi et al. (2002). We here only focused on a simple relationship between the discharge location of hot water to the volcanic edifices and type of hot water chemistry.

As suggested by many geothermal geochemists (e.g. Noda, 1987), the  $\text{SO}_4/\text{Cl}$  and  $\text{SO}_4/\text{HCO}_3$  ratios of hot waters tend to decrease with increasing distance from the volcanic summit. Noda (1987) emphasized that the  $\text{SO}_4/\text{Cl} + \text{SO}_4$  ratio is strongly controlled by the vertical process beneath fumaroles near the summit of volcanoes where rising volcanic gas is primarily dominant in  $\text{CO}_2$  and  $\text{H}_2\text{S}$ , but  $\text{CO}_2$  tends to be liberated to the atmosphere then only  $\text{H}_2\text{S}$  is oxidized as sulfuric acid solely concentrating in hot water.

Fig. 12 shows the relationship between the altitude of hot water discharge and the  $\text{SO}_4/\text{Cl} + \text{SO}_4$  ratio of the hot water in the study area. Usually, we should normalize the altitude into the relative altitude from the base of volcano to the summit. However, the altitudes of monogenetic volcanoes of the Bajawa Breccia Cone Complex are regularly around 1500 m above sea level owing to the uniform genesis and then the absolute altitude can be used. Fig. 12 shows the existence of a uniform proportionality that suggests a uniform hydrological process in slopes to the several directions around the Bajawa Breccia Cone Complex.

Mengeruda hot water is exceptionally large in the  $\text{SO}_4/\text{Cl} + \text{SO}_4$  ratio respective to its low altitude. Considering the exceptionally long distance as far as 12 km from the summit of Inie Like volcano to the Mengeruda hot springs, this is ascribed to the efficient mobility of aquifer by the fault, preserving the higher altitude equilibrium. Actually, the fault was confirmed on the field near the Mengeruda hot springs (Muraoka et al., 2002a).

Nage hot water is characterized by the homogeneity not only on Fig. 12 but also on other components. This is ascribed into the specific hydrological setting of the Nage caldera as a basin. This is distinctive from most of other geothermal systems developed on the volcanic slopes and a relatively voluminous hot water reservoir might be expected as seen in the silica sinter deposits in the area.

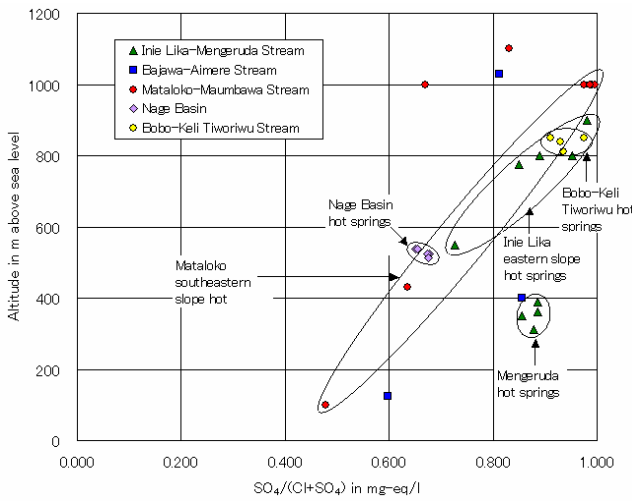


**Figure 12: Relation between the discharge altitude and  $\text{SO}_4/(\text{Cl}+\text{SO}_4)$  ratio in mg-eq/l of hot waters around the Bajawa Breccia Cone Complex.**

## 6. SHALLOW EXPLORATORY WELLS

Three shallow exploratory wells MTL-1, MT-1 and MT-2 have been drilled in the Mataloko geothermal field in this project and their localities are shown in Fig. 13. This project was successfully completed with the flow-test steam production of 15 tons per hour from the well MT-2 at the depth of 162.35 m (Fig. 14; Sueyoshi et al., 2002; Sitorus et al., 2002). After the flow-test, this well was deepened to 182.02 m.

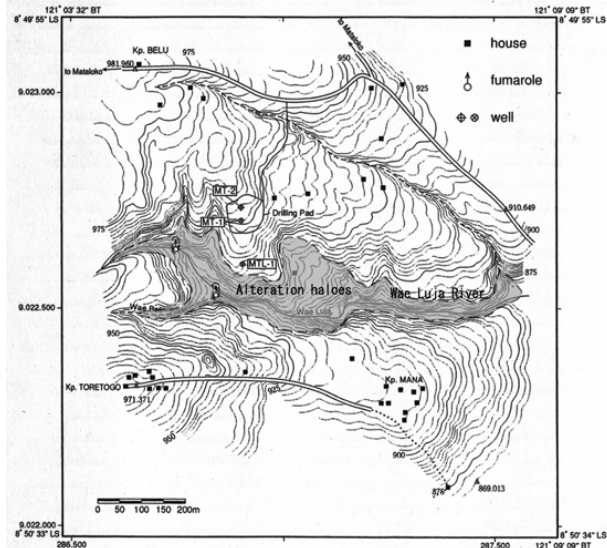


**Figure 13: Locality of the exploratory wells MTL-1, MT-1 and MT-2 (Sueyoshi et al., 2002) and an outline extent of alteration haloes in the Mataloko geothermal field (modified from Akasako et al., 2002).**

However, because of the limited instrumentation in the remote island, the earlier two wells MTL-1 and MT-1 encountered an unexpected blow out of steam at the depths of 103.23 m and 207.26 m, respectively, and the pressure-temperature logging data of the three wells were insufficient to characterize the reservoir condition. Therefore, the supplementary characterization of the Mataloko geothermal reservoir would be attained through the use of available cutting samples. The well MT-1 is the

deepest among the three wells and the most adequate for the mineralogical analyses.

The borehole lithology of the well MT-1 is given by Sueyoshi et al. (2002). The lithology is broadly divided into the lower tuff unit and upper andesite lava - tuff breccia alternation unit. They are probably correlated to the Aimere Scoria Flow Deposits and the Mataloko Andesite that consists of breccia cone-forming phreato-magmatic eruption products, respectively, as shown in the cross sections of Fig. 4. The boundary depth of the two units is difficult to determine accurately from the cutting samples, but is estimated at a depth of 172 m. This is also supported by the relic kaolinite occurrence just below the depth of 172 m.



**Figure 14: Photograph of the flow test of NEDO MT-2 well. It was successful. About 15 tons per hour of dry steam were stably produced at an entirely valve open state. Considering the shallower well depth of 162.35 m, the production rate is quite economical.**

## 7. BOREHOLE MINERALOGY

Based on the X-ray powder examination on the alteration of borehole cuttings of the MT-1 well, we estimated a temperature profile at crystallization stage (Nasution et al., 2003). The details of the works are too verbose to describe here and only the essence is given for the characterization of the Mataloko geothermal system.

The hydrothermal alteration of the MT-1 well is divided into the kaolinite -  $\alpha$ -cristobalite (I) - , zeolite (II) - and kaolinite (III) - zones that are defined at the depth intervals of 0-61 m, 61-172 m and 172-207 m, respectively (Table 1). Zone II is further subdivided into the upper heulandite (IIa) - , middle laumontite (IIb) - and lower wairakite (IIc) - subzones in descending order.

A temperature profile in the crystallization process can be deduced from the phase equilibria of zeolite minerals and the kaolinite crystallinity index. Based on the experimentally determined univariant reactions of zeolite minerals (Liou, 1971; Cho et al., 1987), the phase change temperature is estimated to be 112 °C at the 100 m depth on heulandite to laumontite (Hu/Lm), 135 °C at the 142 m depth on laumontite to yugawaralite (Lm/Yu) and 225 °C at the 166 m depth on yugawaralite to wairakite (Yu/Wa), respectively, which are plotted in Fig. 15. The temperature estimation by the kaolinite crystallinity index on the peak width of 001 reflection in  $2\theta$  degree was proposed by Eckhart and von Gaertner (1962) and Eckhart (1965). It can be applied to the temperature of 200 °C or less.

**Table 1 Mineral constitutions and mineral zoning in the cuttings of the well MT-1, the Mataloko geothermal field, central Flores.**

No	Depth (m)	Lithology	Qz	Cr	Pl	Kf	Sm	Sr	Ch	Ka	S/K/S'	Hu	Es	Yu	Lm	Wa	Ah	Al	Na	Jr	Wd	Gb	Ru	Pv	Hm	Mg	Cc	Px	Zoning
1	0- 10	Tuff breccia	+	+	-	-	-	-	+	-	-	-	-	-	-	-	-	-	-	-	-	-	-	-	-	-	-	-	
2	10- 46	Andesite*	-	++	-	-	+	-	-	+	-	-	-	-	-	-	-	-	-	-	-	-	-	-	-	-	-	Zone-I	
3	46- 49	Andesite*	-	++	-	-	+	-	-	-	?	-	-	-	-	-	-	-	-	-	-	-	-	-	-	-	.....Zone-IIa.....		
4	49- 58	Andesite*	+	+	+	-	++	-	-	-	-	-	-	-	-	-	-	?	-	-	-	-	-	-	-	-	.....Zone-IIb.....		
5	59- 61	Andesite*	-	++	-	-	+	-	-	-	-	-	-	-	-	-	-	-	-	-	-	-	-	-	-	-	.....Zone-IIb.....		
6	61- 100	Andesite*	+	-	+	-	++	-	-	-	-	-	-	-	-	-	-	-	-	-	-	-	-	-	-	-	Zone-IIc		
7	100- 106	Andesite	+	-	+	-	++	-	-	-	-	-	-	-	-	-	-	-	-	-	-	-	-	-	-	-	.....Zone-IIc.....		
8	106- 121	Andesite	+	-	+	-	++	-	-	-	-	-	-	-	-	-	-	-	-	-	-	-	-	-	-	-	Zone-III		
9	121- 127	Andesite*	+	-	++	?	+	-	-	-	-	-	-	-	-	-	-	-	-	-	-	-	-	-	-	-	.....Zone-III.....		
10	127- 142	Tuff breccia**	+	++	?	+	-	-	-	-	-	-	-	-	-	-	-	?	+	+	-	-	-	-	-	-	.....Zone-III.....		
11	142- 160	Tuff breccia	+	+	?	+	-	-	-	-	-	-	-	-	-	-	-	-	-	-	-	-	-	-	-	-	.....Zone-III.....		
12	160- 163	Tuff	+	-	++	-	-	-	-	-	-	-	-	-	-	-	-	-	-	-	-	-	-	-	-	-	.....Zone-III.....		
13	163- 166	Tuff breccia	+	-	+	-	++	-	-	-	-	-	-	-	-	-	-	-	-	-	-	-	-	-	-	-	.....Zone-III.....		
14	166- 172	Tuff	+	-	?	+	-	-	-	-	-	-	-	-	-	-	-	-	-	-	-	-	-	-	-	-	.....Zone-III.....		
15	172- 184	Tuff	+	-	+	-	++	-	-	-	-	-	-	-	-	-	-	-	-	-	-	-	-	-	-	-	.....Zone-III.....		
16	184- 190	Tuff	+	-	+	-	++	-	-	-	-	-	-	-	-	-	-	-	-	-	-	-	-	-	-	-	.....Zone-III.....		
17	190- 207	Tuff	++	-	+	-	++	-	-	-	-	-	-	-	-	-	-	-	-	-	-	-	-	-	-	-	.....Zone-III.....		

Qz, quartz; Cr,  $\alpha$ -cristobalite; Pl, plagioclase; Kf, K-feldspar; Sm, smectite; Sr, sericite; Ch, chlorite; Ka, kaolinite; S/K, smectite/ kaolinite mixed-layer clay mineral; S/S, smectite/ sericite mixed-layer clay mineral; Hu, heulandite; Es, epstilite; Yu, yugawaralite; Lm, laumontite; Wa, wairakite; Ah, anhydrite; Al, alunite; Na, natroalunite; Jr, jarosite; Wd, woodhouseite; Gb, gibbsite; Ru, rutile; Py, pyrite; Hm, hematite; Mg, magnetite; Cc, calcite and Px, pyroxene.

++, very abundant; +, fairly abundant; +, subordinate and -, existent.

\*, includes tuffaceous fragments and \*\*, includes andesitic lava fragments.

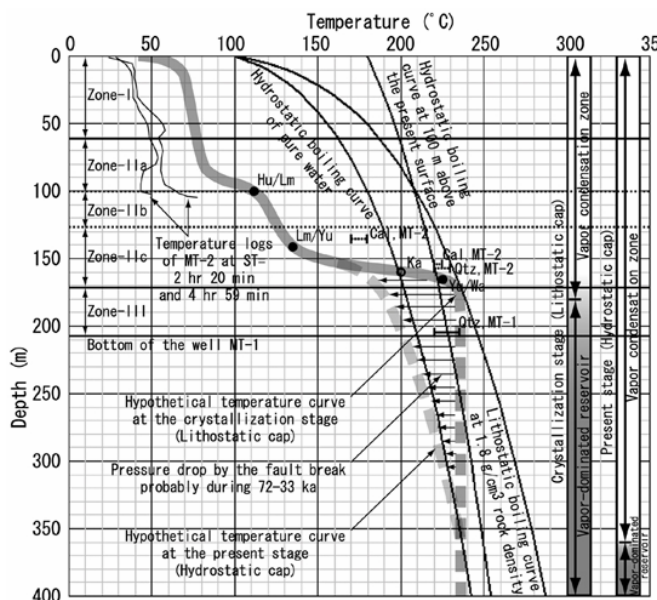


**Figure 15: Summary of the temperature regimes in the Mataloko geothermal system. Temperature logging data of the well MT-2 are given by Sueyoshi et al. (2002). Lateral bars indicate homogenization temperatures of fluid inclusions by Sawaki and Muraoka (2002). Cal, calcite; Qtz, quartz; Hu, heulandite; Lm, laumontite; Yu, yugawaralite; Wa, wairakite.**

Although kaolinite is lack in Zone-II, a temperature of 200 °C was estimated to be about 160 m depth from the regression line extrapolated from those of Zone-I and Zone-III. This temperature (Ka) is also plotted in Fig. 15. The thermal regime of the Mataloko geothermal system is evaluated here by comparing its data with other available data. Figure 15 summarizes all the available data, not only from the well MT-1 but also from MT-2. Only kaolinite and the accompanying sulfate minerals in Zone-III are considered as relic minerals on their origins but kaolinite might have also been re-equilibrated in the major crystallization stage. All the mineralogical data such as the zeolite phase relationship and the kaolinite crystallinity index consistently indicate a “hypothetical temperature curve at the crystallization stage” as given in Fig. 15. This hypothetical curve clearly exceeds the hydrostatic boiling-point curve of pure water in Subzone-IIc and Zone-III, the

maximum of which is close to the lithostatic boiling-point curve at a rock density of 1.8 g/cm<sup>3</sup>. Sawaki and Muraoka (2002) reported a several homogenization temperature data of fluid inclusions in quartz and calcite from the wells MT-1 and MT-2 (Fig. 15). Their data are consistent with the hypothetical temperature curve and confirm the mineralogical temperature estimate. Fluid inclusion data are empirically known to show nearly a modern hydrothermal temperature regime, and therefore, the hypothetical curve may represent a very recent temperature regime in the Mataloko geothermal system. To explain such the high temperature conditions, Sawaki and Muraoka (2002) speculated that surface units of 100 m thickness were eroded off after the formation of the fluid inclusions as a 100 m upward boiling-point curve (Fig. 15). However, based on the mineralogical study, it is noted that the high temperature gradient intervals of the hypothetical temperature curve coincided well with the zones of prevalent clay minerals, possibly having formed an almost impermeable clay cap. This might have played the role of the lithostatically-pressurized cap that has bounded a lower vapor-dominated reservoir and upper vapor condensation zone. The hypothetical curve, in fact, reaches 236 °C at a depth around 180 m which is ascribed to the maximum enthalpy point on the two-phase region of water, because the pressure of the lithostatic boiling-point curve at a rock density of 1.8 g/cm<sup>3</sup> reaches 31.8 kg/cm<sup>2</sup> (32.4 bar) at the depth of around 180 m, that is, the known pressure of the maximum enthalpy point (White et al., 1971).

The mineralogical temperature profile thus indicates that the Mataloko reservoir had, at least once, experienced a vapor-dominated reservoir up to a very shallow depth. The vapor condensation zone above the vapor-dominated reservoir generally has a thickness of 360 m (White et al., 1971), but it has only a half of that in the Mataloko area at the time of crystallization. Abundant clay and zeolite minerals in Zone-II might have formed an extremely impermeable zone and the continuing excess heat supply might have generated a lithostatically pressurized clay cap for the rock density of 1.8 g/cm<sup>3</sup>.

The hypothetical temperature curve may represent a very recent temperature regime in the Mataloko geothermal system, as supported by the fluid inclusion data. Nevertheless, Sitorus et al. (2002) reported that the maximum temperature and pressure of the well MT-2, 35 m north of the well MT-1, was 192.30 °C and 13.86 bar at a

depth of 175 m. These pressure-temperature conditions are far less than those of the vapor-dominated system (White et al., 1971). Although they were not measured in the same well, it is most likely that the lithostatically pressurized clay cap of the well MT-1 has very recently been liberated by the break of the WNW-ESE trending Wae Luja fault (Akasako et al., 2002) and the present temperature regime in the Mataloko geothermal system may have somewhat declined to the “hypothetical temperature curve at the present stage” as shown in Fig. 15. This possibility is strongly supported by Muraoka et al. (2002a) that many conjugate sets of the WNW-ESE and ENE-WSW strike-slip type faults are detected near the Bajawa rift zone on the satellite image and their origin may be ascribed to the recent dike filling beneath the Bajawa rift zone because their local E-W contraction stress field is incompatible with the regional N-S contraction stress regime. Based on this idea, the fault break and the resulting pressure drop are considered to have occurred after most of the Bajawa Breccia Cone Complex (dike fillers) appeared and before most of surface alterations took place. Because the former is dated to be 160-72 ka and the latter is dated to be 33-0 ka by the thermoluminescence method by Takashima et al. (2002), the fault break and the resulting pressure drop might be estimated to have occurred during 72-33 ka.

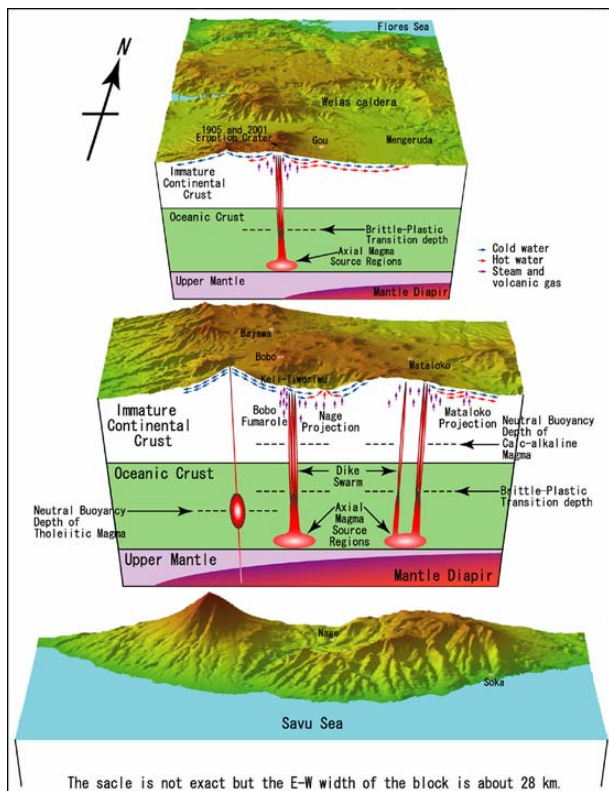


**Figure 16: A generalized model of magmatic and geothermal systems in the Bajawa rift zone.**

Normally, such a recent temperature decline should also have been recorded in the mineral equilibria and fluid inclusions, but this has not actually been recorded. This could be explained by the vapor-dominated nature itself that Subzone-IIc and Zone-III have already been filled with dry steam at the time of the fault break and the water-rock interaction was limited. This also suggests that the thickness of the vapor condensation zone was instantaneously raised to 360 m by the fault break but the vapor-dominated reservoir could still be preserved until present beneath the thickened vapor condensation zone as

observed in the single-phase dry steam discharge during the flow test of the well MT-2 (Matsuda et al., 2002).

## 8. INTEGRATION AND SUMMARY

The Flores to Pantar segment forms en echelon volcanic islands that are partly explained by the NNW-SSE shear stress accommodated between the stable Sundaland and the north-moving Australia continent. However, the spatial overlap of the anticline of volcanic basement and overlying younger volcanoes in each element of en echelon structure requires another explanation. This might be ascribed to a linkage of both processes by the concept of mantle diapirs. The hypothesis of mantle diapirs that can be passively deformed by the active deformation of the overlying brittle layer, also explains the reason why the spacing of volcanoes abruptly reduces in the Flores to Pantar segment respective to that in the western Indonesia. Western Indonesia is comparable with the situation before the deformation in Fig. 6B, whereas the Flores to Pantar segment is comparable with that after the deformation in Fig. 6B.

From the geological aspect, one of the most important results is that the Bajawa rift zone was recognized in the area. It contains about sixty monogenetic volcanoes along the rift zone 10 km wide and 20 km long, and these volcanic rocks consist of calc-alkaline andesite that is very homogeneous respective to their scattered distribution. The phreato-magmatic eruption occurred near the summit of Inie Lika volcano along the rift zone on January 2001 and formed an NNW-SSE trending fissure, about 20 m wide and 300 m long (Muraoka et al., 2002b). This event suggests that the upper tip of a magmatic dike might have risen near by the ground surface as shown in the simple deformation model (Muraoka et al., 2002b). Therefore, it seems evident that the Bajawa rift zone is formed by the subsurface dike swarm system (Fig. 16). The phase equilibria of chemistry of the volcanic rocks suggest that the magmatic dike swarm may be derived from the bottom of oceanic crust (Fig. 16).

Geothermal manifestations in the Bajawa field are represented by the three steaming grounds in the Bobo, Nage and Mataloko areas and one voluminous hot spring discharge in the Mengeruda area. Bobo and Mataloko are situated at relatively high altitude and a steam-condensate or steam-heated fluid type geothermal system (Fig. 16). Considering the prevailing acid clay alteration zone and excess heat supply, they probably form a vapor-dominated geothermal system at a depth. Nage is situated in the bottom of Nage caldera that hydrologically tends to form the shallower water table and a water dominated geothermal system at a depth (Fig. 16). Homogeneity of the hot water and silica sinter deposits in the Nage area support this possibility. Mengeruda is 12 km away from Inie Lika volcano (Fig. 16) but still dominant in the sulfate component that is explained by the E-W trending strike-slip faults.

Regardless of these manifestations, most areas of the Bajawa rift zone seem quite prospective on the geothermal potential, because of the ubiquitously shallow heat sources and uniform hydrological settings.

## REFERENCES

Akasako, H., Matsuda, K., Tagomori, K., Koseki, T., Takahashi, H. and Dwipa, S.: Conceptual models for geothermal systems in the Wolo Bobo, Nage and Mataloko fields, Bajawa area, central Flores,

Indonesia, Bull. Geol. Surv. Japan, 53, (2002), 375-387.

Baker, D.R. and Eggler, D.H.: Fractionation paths of Atka (Aleutians) high-alumina basalts: constraints from phase relations, J. Volcanol. Geotherm. Res., 18, (1983), 387-404.

Baker, D.R. and Eggler, D.H.: Compositions of anhydrous and hydrous melts coexisting with plagioclase, augite, and olivine or low-Ca pyroxene from 1 atm to 8 kbar: Application to the Aleutian volcanic center of Atka, American Mineralogist, 72, (1987), 12-28.

Cho, M., Maruyama, S. and Liou, J. M.: An experimental investigation of heulandite-laumontite equilibrium at 1000-2000 bar Pfluid, Contrib. Mineral. Petrol., 97, (1987), 43-50.

Curry, J.R., Shor Jr, G.G., Raiit, R.W. and Henry, M.: Seismic refraction and reflection studies of crustal structure of the eastern Sunda and western Banda arcs, J. Geophys. Res., 82, (1977), 2479-2489.

Eckhart, F. J. and von Gaertner, H. R.: Zur entstehung und umbildung der kaolin-kohlentonsteine, Fortsch. Geol. Rheinl. Westf., 3, (1962), 624-640.

Eckhart, F. J.: Über den einfluss der temperaturen auf den kristallographischen ordnungsgrad von kaolinit, Proc. Int. Clay Conf. (Stockholm), 3, (1965), 137-145.

Kreemer, C., Holt, W.E., Goes, S. and Govers, R.: Active deformation in eastern Indonesia and the Philippines from GPS and seismicity data, J. Geophys. Res., 105, (2000), 663-680.

Liou, J. G.: P-T stabilities of laumontite, wairakite, lawsonite and related minerals in the system CaAl<sub>2</sub>Si<sub>2</sub>O<sub>8</sub>-SiO<sub>2</sub>-H<sub>2</sub>O, Jour. Petrol., 12, (1971), 379-411.

Matsuda, K., Sriwana, T., Primulyana, S. and Futagoishi, M.: Chemical and isotopic studies of well discharge fluid of the Mataloko geothermal field, Flores, Indonesia, Bull. Geol. Surv. Japan, 53, (2002), 343-353.

Miyashiro, A.: Volcanic rock series in island arcs and active continental margins, Amer. J. Sci., 274, (1974), 179-218.

Muraoka, H.: Exploration on geology and gold ore deposits in the Lesser Sunda Islands, southern sea, Chishitsu (Geological) News, No.423, (1989), 35-42 (in Japanese).

Muraoka, H.: Conceptual model for emplacement depth of magma chambers and genesis of geothermal systems, Proc. 30th Int'l. Geol. Congr., Beijing, 9, (1997), 143-155.

Muraoka, H. and Takakura, S.: Explanatory text of the geological map of Hakkoda Geothermal Area, scale 1:100,000, Miscellaneous Map Series (21-4), Geol. Surv. Japan, (1988), 27p (in Japanese with English abstract).

Muraoka, H., Uchida, T., Sasada, M., Yagi, M., Akaku, K., Sasaki, M., Yasukawa, K., Miyazaki, S.-I., Doi, N., Saito, S., Sato, K. and Tanaka, S.: Deep geothermal resources survey program: igneous, metamorphic and hydrothermal processes in a well encountering 500 °C at 3729 m depth, Kakkonda, Japan, Geothermics, 27, (1998), 507-534.

Muraoka, H., Nasution, A., Urai, M., Takahashi, M., Takashima, I., Simanjuntak, J., Sundhoro, H., Nanlohy, F., Sitorus, K., Takahashi, H. and Koseki, T.: Tectonic, volcanic and stratigraphic geology of the Bajawa geothermal field, central Flores, Indonesia, Bull. Geol. Surv. Japan, 53, (2002a), 109-138.

Muraoka, H., Yasukawa, K., Urai, M., Takahashi, M., Nasution, A. and Takashima, I.: 2001 fissure-forming eruption of Inie Lika Volcano, central Flores, Indonesia, Bull. Geol. Surv. Japan, 53, (2002b), 175-182.

Muraoka, H., Nasution, A., Urai, M., Takahashi, M. and Takashima, I.: Geochemistry of volcanic rocks in the Bajawa geothermal field, central Flores, Indonesia, Bull. Geol. Surv. Japan, 53, (2002c), 147-159.

Nasution, A., Muraoka, H., Rani, M., Takashima, I., Takahashi, M., Akasako, H., Matsuda, K. and Badrudin, M.: Geothermal prospects of Flores Island in Indonesia viewed from their volcanism and hot water geochemistry, Bull. Geol. Surv. Japan, 53, (2002), 87-97.

Nasution, A., Taniguchi, M., Kikuchi, T. and Muraoka, H.: A lithostatically pressurized clay cap of the vapor-dominated reservoir deduced from hydrothermal alterations of borehole cuttings in the Mataloko geothermal field, Flores Island, eastern Indonesia, J. Geotherm. Res. Soc. Japan, 25, (2003), 193-210.

Noda, T.: Anion index as an indicator of geothermal activity, J. Geotherm. Res. Soc. Japan, 9, (1987), 133-141.

Rutherford, E., Burke, K. and Lytwyn, J.: Tectonic history of Sumba Island, Indonesia, since the Late Cretaceous and its rapid escape into the forearc in the Miocene, Journal of Asian Earth Sciences, 19, (2001), 453-479.

Sawaki, T. and Muraoka, H.: Fluid inclusion study on wells MT-1 and MT-2 in the Mataloko geothermal system, Indonesia, Bull. Geol. Surv. Japan, 53, (2002), 337-341.

Sitorus, K., Sulistyohadi, F. and Simanjuntak, J.: Long term flow test of the MT-2 well, the Mataloko geothermal field, Ngada, Flores Island, Indonesia, Bull. Geol. Surv. Japan, 53, (2002), 389-397.

Sueyoshi, Y., Matsuda, K., Shimoike, T., Koseki, T., Takahashi, H., Futagoishi, M., Sitorus, K. and Simanjuntak, J.: Exploratory well drilling and discharge test of wells MT-1 and MT-2 in the Mataloko geothermal field, Flores, Indonesia, Bull. Geol. Surv. Japan, 53, (2002), 307-321.

Takahashi, M., Urai, M., Yasukawa, K., Muraoka, H., Matsuda, K., Akasako, H., Koseki, T., Hisatani, K., Kusnadi, D., Sulaeman, B. and Nasution, H.: Geochemistry characteristics of hot spring water at Bajawa area, central Flores, Indonesia, Bull. Geol. Surv. Japan, 53, (2002), 183-199.

Takashima, I., Nasution, A. and Muraoka, H.: Thermoluminescence dating of volcanic and altered rocks in the Bajawa Geothermal Area, central Flores Island, Indonesia, Bull. Geol. Surv. Japan, 53, (2002), 139-146.

Tatsumi, Y.: Migration of fluid phases and genesis of basalt magmas in subduction zones, J. Geophys. Res., 94, (1989), 4697-4707.

Tomiya, A.: Volume of mantle diapir compatible with life span of a typical island-arc volcano, Bull. Volcanol. Soc. Japan, 36, (1991), 211-221 (in Japanese with English abstract).

Vail, P.R. and Hardenbol, J.: Sea-level changes during the Tertiary, Oceanus, 22, (1979), 71-79.

Walker, G.P.L.: Volcanic rift zones and their intrusion swarms, J. Volcanol. Geotherm. Res., 94, (1999), 21-34.

White, D.E., Muffler, L.J.P. and Truesdell, A.H.: Vapor-dominated hydrothermal systems compared with hot-water systems, Econ. Geol., 66, (1971), 75-97.